Main Group Chemistry Hot Paper

How to cite: *Angew. Chem. Int. Ed.* **2021**, *60*, 21761–21766
International Edition: doi.org/10.1002/anie.202104341
German Edition: doi.org/10.1002/ange.202104341

Cycloadditions with a Stable Charge-Separated Cyclobutadiene-Type Amido-Substituted Silicon Ring Compound

Jan Keuter, Alexander Hepp, Constantin G. Daniliuc, Milica Feldt, and Felicitas Lips**

Dedicated to Prof. F. Ekkehardt Hahn on the occasion of his 66th birthday

Abstract: *Reductive debromination of {N(SiMe$_3$)$_2$}SiBr$_3$ with Rieke magnesium results in the formation of the five-vertex silicon cluster with one bromine substituent Si$_5${N(SiMe$_3$)$_2$}$_5$Br,* ***1****, and the cyclobutadiene analogue* ***2*** *in a 1:1 ratio. The latter features a planar four-membered silicon ring with a charge-separated electronic situation. Two silicon atoms in* ***2*** *are trigonal planar and the other two trigonal pyramidal. In cycloadditions with ethylene, diethylacetylene, 1,5-cyclooctadiene, and 2,3-dimethyl-1,3-butadiene cyclic unsaturated ring compounds (****3****–****6****) were formed at room temperature in quantitative reactions. Two of the products (****3*** *and* ***6****) show photochemical isomerization with LED light (λ = 405 nm) to afford saturated ring compounds* ***4e*** *and* ***6′****.*

Cyclobutadiene represents one of the most intriguing unsaturated hydrocarbon ring compounds that is defined by antiaromaticity, ring strain, and difficulties in its preparation.[1–3] Cyclobutadiene was synthesized after several attempts by oxidative degradation of cyclobutadiene iron tricarbonyl with ammonium cerium(IV) nitrate. When the cyclobutadiene ring is released from the iron complex it reacts with electron-deficient alkynes to yield Dewar benzene ring compounds.[4–6] Moreover, cyclobutadiene is reported to be used as a ligand in catalysis.[7]

The synthesis and characterization of heavier analogues of cyclobutadiene, for instance with the element silicon, likewise represents a challenging task. Planar neutral four-membered unsaturated silicon rings were only realized in a few examples by using a bulky aryl substituent and with a combination of an amine and an amidinato ligand. With aryl substituents the ring in **A** has a rhombic shape and the silicon atoms display a charge-separated electronic situation with alternating trigonal planar and trigonal pyramidal coordinated silicon atoms (Figure 1).[8] With amine and amidinato substituents electron delocalization of σ-, π- and non-bonding electrons was observed in the four-membered ring compound Si$_4$L$_2${N(SiMe$_3$)Dipp}$_2$ **B** (L = PhC(N*t*Bu)$_2$, Figure 1).[9] If only the amine substituent {N(SiMe$_3$)Dipp} was used to stabilize the silicon ring, a folded bicyclic ring **C** was obtained.[10] Due to the instability of **A** in solution, the reactivity of the planar four-membered unsaturated silicon ring compounds was only investigated for **B** in a reaction with sulfur.[9]

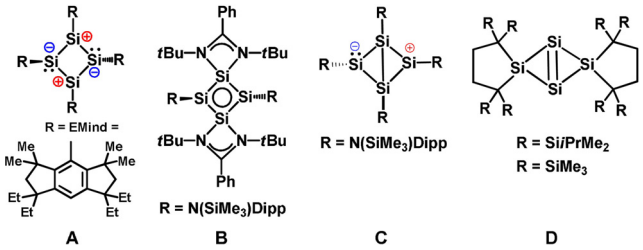

Figure 1. Unsaturated silicon ring compounds (Dipp = 2,6-*i*Pr$_2$C$_6$H$_3$).

Another unsaturated ring compound with a rhombic Si$_4$ ring includes the tetrasilicon analogue of a bicyclo[1.1.0]but-1(3)-ene **D** (Figure 1).[11] This compound with R = SiMe$_3$ reacts with iodine to afford a planar silicon ring structure with π-type single bonding between the bridgehead silicon atoms.[12] Furthermore, reactions with carbon tetrachloride and methanol to afford saturated tetrasilane species were observed.[13]

A square planar tetrasilacyclobutadiene unit with silyl substituents has also been reported as a transition metal complex.[14,15] Further silicon ring compounds with planar four-membered silicon rings are dicationic like [Si$_4$L$_2$(SiLCl)$_2$]$^{2+}$ and [(LSi)$_4$]$^{2+}$ (L = PhC(N*t*Bu)$_2$).[16,17]

Herein, we report on the reductive debromination of {N(SiMe$_3$)$_2$}SiBr$_3$[18] with 1.5 equiv of activated magnesium (Mg*)[19] that yields a saturated bromo-substituted pentaamidopentasilane **1** and an unsaturated amido-substituted silicon ring compound **2** with a planar rhombic Si$_4$ ring in a 1:1 ratio (Figure 2). Separation of **1** and **2** can be achieved using fractional crystallization in toluene or *n*-hexane. The crystallization of **1** is preferred when the reaction residue is

[*] M. Sc. J. Keuter, Dr. A. Hepp, Dr. F. Lips
Westfälische Wilhelms-Universität Münster
Institut für Anorganische and Analytische Chemie
Corrensstrasse 28–30, 48149 Münster (Germany)
E-mail: lips@uni-muenster.de
Dr. C. G. Daniliuc, Dr. M. Feldt
Westfälische Wilhelms-Universität Münster
Organisch Chemisches Institut and
Center for Multiscale Theory and Computation
Corrensstrasse 36, 48149 Münster (Germany)
E-mail: mfeldt@uni-muenster.de
Supporting information and the ORCID identification number(s) for the author(s) of this article can be found under: https://doi.org/10.1002/anie.202104341.

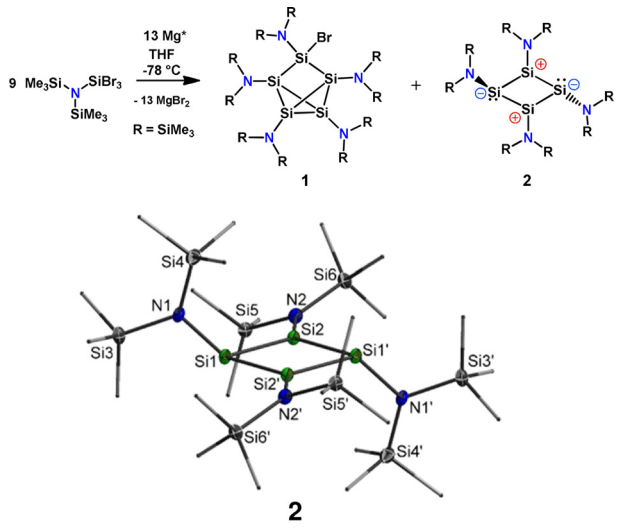

Figure 2. Top: Synthesis of **1** and **2**. Bottom: Molecular structures of **2** (thermal ellipsoids set at 50 % probability level). Selected distances [Å] and angles [°]: Si1–Si2 2.282(7), Si1–Si2′ 2.280(7), Si2···Si2′ 2.800(1), Si1···Si1′ 3.602(1), Si1–N1 1.7617(17), Si2–N2 1.7333(16); Si2-Si1-Si2′ 75.72(3), Si1-Si2-Si1′ 104.28(3).

extracted in *n*-hexane and the crystallization of **2** when using toluene at the same step. Each of the silicon atoms in the folded four-membered ring in **1** is connected to one amido substituent. This Si_4 ring is capped by an $\{N(SiMe_3)_2\}BrSi$ unit. One possible formation pathway for **1** is a cycloaddition of the transient silylene $\{N(SiMe_3)_2\}BrSi$: with the planar Si_4 ring of **2**.

In **2**, the silicon ring has a rhombic shape and an inversion center in the middle of the Si_4 ring. The Si1−Si2 (2.282(7) Å) and Si1−Si2′ (2.280(7) Å) bond lengths are in the range between single (2.34 Å) and double bonds (2.21 Å).[20] Two opposite silicon atoms (Si2 and Si2′) have a trigonal planar configuration with sum of the surrounding bond angles of 359.99(2)°. The other two silicon atoms (Si1 and Si1′) in the ring have a trigonal pyramidal environment with sum of surrounding bond angles of 323.27(2)°.

This was also the case in **A**, which features a charge-separated electronic situation. The chemical shifts of the two distinct silicon atoms appear in the downfield region at 258.9 ppm for the trigonal planar atoms and in the highfield region at −85.9 ppm for the pyramidal atoms in the ^{29}Si NMR spectrum recorded in C_6D_6 at 300 K. Similar chemical shifts were detected in $[D_8]$THF (258.6 and −85.9 ppm, respectively). Thus the difference between these chemically and magnetically different silicon atoms is $\Delta\delta = 344.8$ ppm. This is in the range of that observed for **A** (350–360 ppm) determined in the solid state. However, in contrast to the EMind-substituted species **A**, variable-temperature ^1H NMR spectra of **2** in $[D_8]$THF demonstrate that no valence tautomerization (interconversion between two rhombic structures) takes place or that this process for **2** has an activation barrier higher than 14.3 kcal mol^{-1}.[21] Furthermore, different to **A**, compound **2** is stable in C_6D_6 at least for two weeks.

Our computational investigations on $Si_4\{N(CH_3)_2\}_4$ species demonstrated that the isomer corresponding to **2** with C_{2h} symmetry is lower in energy than species with a folded Si_4 ring in C_{2v} symmetry (short bond isomer) and D_{2d} symmetry (long bond isomer).[10] These calculations were reinvestigated with $N(SiH_3)_2$ and $N(SiMe_3)_2$ substituents. They showed that the isomers with folded Si_4 rings are up to 5.6 kcal mol^{-1} higher in energy for the $N(SiH_3)_2$ substituents and up to 6.7 kcal mol^{-1} for the $N(SiMe_3)_2$ substituent (Page S64).

The electronic structure of **2** was investigated with DFT calculations (see Supporting Information for details). Figure 3

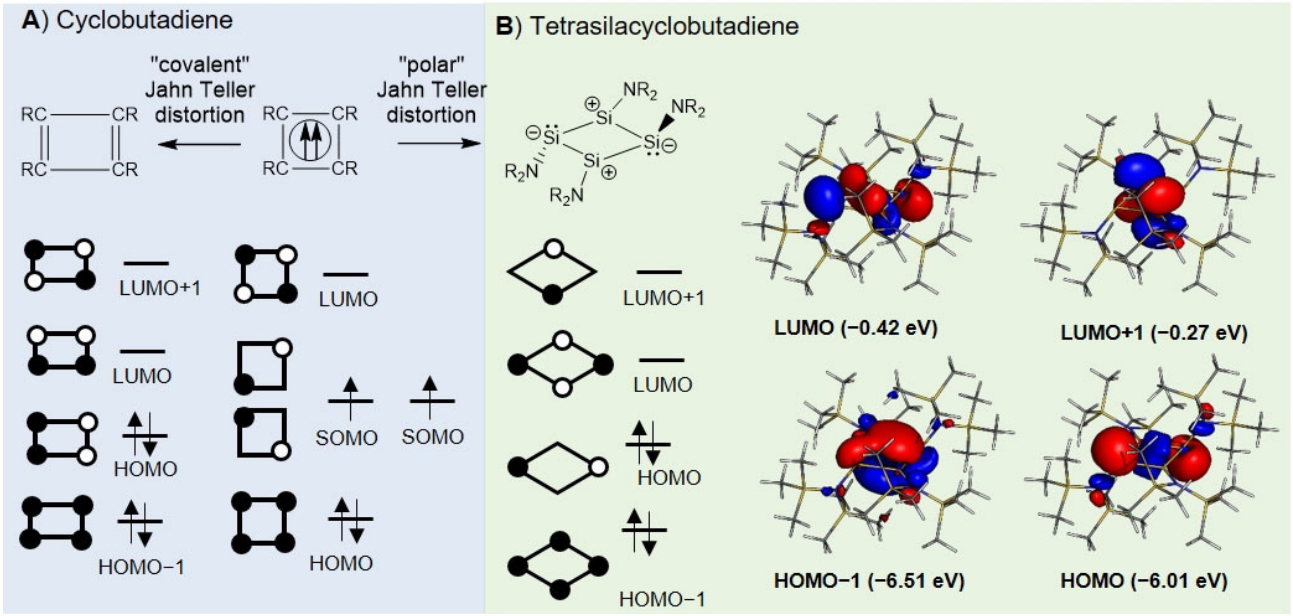

Figure 3. A) Schematic orbital diagram of the π electrons in rectangular and square planar cyclobutadiene species (C_4R_4). B) Kohn–Sham molecular orbitals of **2** (CAM-B3LYP-D3(BJ)/def2-QZVP, isovalue set at ±0.04 a.u.) with schematic representation of the MOs.

shows the molecular orbitals of the four π-electrons of **2** calculated using CAM-B3LYP-D3(BJ)/def2-QZVP[22] (isovalue set at ±0.04 a.u.). The HOMO−1 includes coefficients of π-symmetry distributed over the entire Si_4 ring representing the in-phase bonding combination of the four π-electrons in **2**. The HOMO of **2** includes an out-of-phase orbital where two p-orbitals at the pyramidal Si atoms are oriented in one direction to enable some kind of small in-phase bonding interaction with their back lobes. The LUMO represents the antibonding combination of all p-orbitals with two nodal planes. The LUMO+1 represents a π*-type orbital with empty p-orbitals at the trigonal planar silicon atoms. Compared to the molecular orbitals of **A**, the sequence of the LUMO and LUMO+1 of **2** appears in opposite order. But the polar Jahn–Teller distortion observed in **A** also occurs in **2** (Figure 3B). This is in contrast to the "covalent" Jahn–Teller distortion observed in cyclobutadiene that transforms the square planar structure in the excited triplet state into the rectangular ring in singlet state with localized C=C double bonds and results in antiaromaticity (Figure 3A).

Moreover, a complete active space self-consistent field (CASSCF) calculation[23] was performed with **2** considering an (8,8) active space. For this calculation a triple-zeta (cc-pVTZ) basis set was employed for all atoms and resulted in occupation numbers of 1.886 and 0.107 for the highest occupied natural orbital (HONO) and the lowest unoccupied natural orbital (LUNO), respectively. These occupation numbers indicate no diradical character ($Y = 11\,\%$)[24] on the silicon atoms in **2** (Pages S52, S53). Furthermore, the calculated differences in Gibbs free energy of **2** in the singlet and the triplet state ($\Delta G = 16.6\ kcal\,mol^{-1}$) and between the closed-shell and open-shell singlet states ($\Delta G = 16.2$ kcal mol^{-1}) are rather high (Table S23). This further confirms the absence of diradical character in **2**. We note that a rather low diradicaloid character was reported for **A**.

To further analyze the nature of the rhombic four-membered silicon ring in **2**, we applied natural bond orbital analysis.[25] This revealed that the trigonal planar Si2 atoms have a remarkable higher positive partial charge of +0.90 than the trigonal pyramidal Si1 atoms with positive partial charges of +0.28. This demonstrates a formal charge-separated bonding situation in **2**. The charge difference (0.62) between the differently configurated silicon atoms is in the range of that observed for **A** (0.47–0.50). Analysis of Mayer[26] bond orders of **2** reflects the multiple bond character in the Si–Si bonds (B.O. 1.12) of the planar rhombic Si_4 ring. The transannular Si···Si distances have significantly lower bond orders of 0.38 and 0.28 and indicate very weak transannular interactions. The Si–N bonds are in the range of single bonds (1.05/0.95). This is in accord with the observed bond lengths (Si1–N1 1.762(2) Å, Si2–N2 1.733(2) Å) and can be explained with the fact that the amido substituents at Si2 and Si2′ are oriented out of the Si_4 ring plane.

The UV/Vis spectrum of **2** shows absorption maxima in *n*-hexane at 345 nm ($\varepsilon = 2402\ L\,mol^{-1}\,cm^{-1}$) and a shoulder occurring at 375 nm ($\varepsilon = 1698\ L\,mol^{-1}\,cm^{-1}$, Figure S6). The UV/Vis spectrum in THF reveals an absorption maximum at 345 nm ($\varepsilon = 1790\ L\,mol^{-1}\,cm^{-1}$). In toluene two clear absorption maxima were found at 352 nm ($\varepsilon = 2408\ L\,mol^{-1}\,cm^{-1}$) and 377 nm ($\varepsilon = 2382\ L\,mol^{-1}\,cm^{-1}$). With TD-DFT calculations in toluene (CAM-B3LYP[22a]/def2-TZVP) we found that the latter two absorption maxima correspond to the HOMO→LUMO excitation at $\lambda = 370$ nm and the HOMO−1 to LUMO+1 transition at $\lambda = 338$ nm. In all three solvents a tailing into the visible region is observed producing a red color. This is probably related to less intensive transitions such as HOMO−2→LUMO mixed with HOMO−1→LUMO+1 at 394 nm according to TD-DFT calculation in toluene (Figure S69).

Different to compound **A**, the high stability of **2** in benzene allowed us to investigate its reactivity. Compound **2** does not react with dihydrogen at room temperature and elevated temperatures of 80 °C. But **2** reacts very selectively in quantitative reactions with alkenes and alkynes such as ethylene, diethylacetylene, 2,3-dimethyl-1,3-butadiene, and 1,5-cyclooctadiene in benzene at room temperature within a few hours to several days. The reaction with ethylene occurs in a [2+2] cycloaddition under formation of bicyclo-[2.2.0]tetrasilacyclohexene **3**. By contrast, the reaction with diethylacetylene proceeds differently and results in compound **4** with a benzvalene-type Si_4C_2 structural motif. In the literature a tetrasilabenzvalene was reported as a product from the reaction of dibromobenzene and a tetrasilacyclobutadiene dianion. The thermodynamically more stable tetrasilabenzvalene was assumed to be formed after isomerization from a tetrasila Dewar benzene derivative.[27,28]

With 1,5-cyclooctadiene a tricyclic ring compound **5** with a saturated Si_4C_2 structural motif and a folded Si_4 unit was observed after eight days. In this reaction only one C=C double bond of the alkene reacted with **2**. The other one is still available in the product for further manipulations. When 2,3-dimethyl-1,3-butadiene was used in the cycloaddition the bicyclic tetrasila-bicyclo-octadiene species **6** was formed in a [4+2] cycloaddition (Scheme 1).[29]

To understand the formation of either bicyclic or tricyclic products in the cycloadditions of **2** with alkenes and alkynes, we investigated the formation of **3** and **4** with DFT methods (see Supporting Information for details). For both reactions two different mechanistic scenarios were considered. The first involves the [2+2] cycloaddition between **2** and the reagent to the bicyclic product and a subsequent rearrangement to the tricyclic species. The second includes a direct formation of the tricyclic product from the reactant complex (Scheme 2 and Scheme 4).

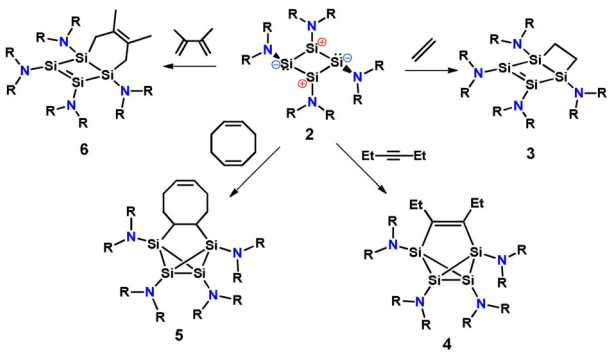

Scheme 1. Cycloadditions with **2** at room temperature (R = $SiMe_3$).

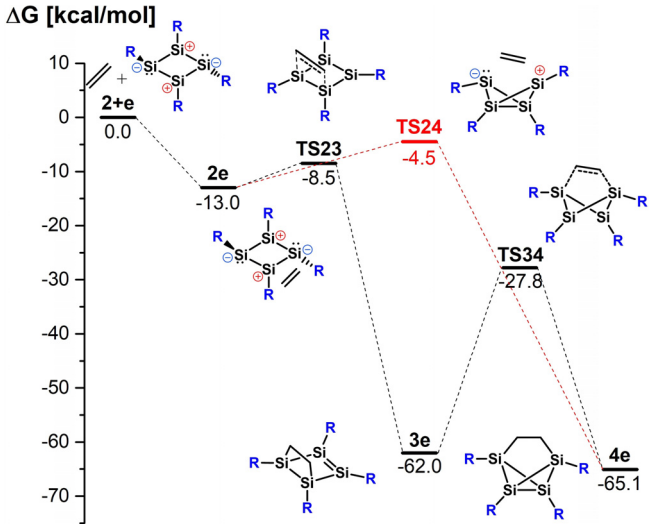

Scheme 2. DFT-calculated mechanism for the formation of **3**.

We found that in the mechanism with ethylene a low activation barrier of only 4.5 kcal mol^{-1} leads from the reactant complex **2e** via **TS23** to the isolated product **3e** in an exergonic reaction. By contrast, the activation barrier to **TS24** with a folded zwitterionic Si_4 ring to reach the tricyclic product **4e** is much higher (8.5 kcal mol^{-1}), which makes this pathway unfavorable.

In the mechanism with diethylacetylene the [2+2] cycloaddition results in the formation of Dewar benzene type intermediate **3h** in an exergonic reaction via transition state **TS23** with a low activation barrier of only 4.2 kcal mol^{-1} (Scheme 3, Pages S68–S72). This Dewar benzene derivative **3h** has a conformer **3h′** that is 6.6 kcal mol^{-1} higher in energy and differs in the orientation of one ethyl group (Page S75). The barrier from **3h′** via **TS34** only amounts to 25 kcal mol^{-1} and thus leads in this case to the thermodynamically more stable isolated product **4h**.

For the second scenario the reactant complex **2h′** has a slightly more zwitterionic character in the Si_4 ring compared

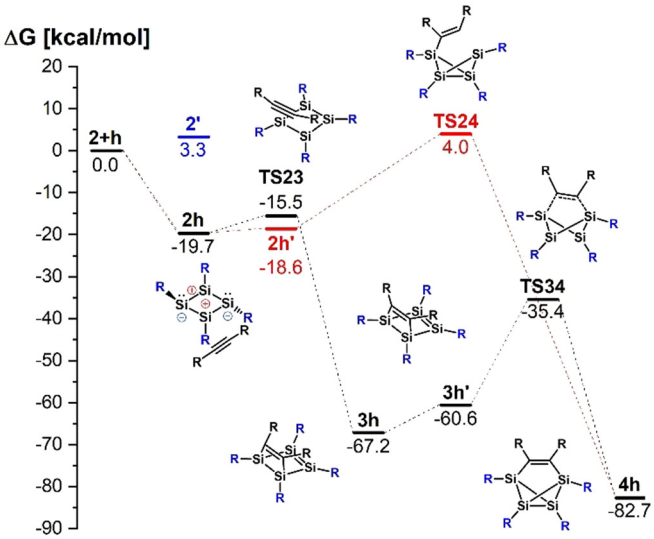

Scheme 3. DFT-calculated mechanism for the formation of **4** (R = Et).

to **2h** (Figure S74, Table S20). However, the formation of **4h** via **TS24** is unfavorable due to the higher activation barrier of 15 kcal mol^{-1} in comparison to only 4.2 kcal mol^{-1} to reach **3h**. In this case, we also considered the addition of diethylacetylene to the folded isomer **2′** (Page S69). However, this is not expected to proceed, because the orientation of the amine substituents hinders the approach of the bulky diethylacetylene substrate to the silicon ring atoms (Figure S74).

To experimentally confirm the calculated mechanism, we performed time-dependent multinuclear NMR spectroscopy during the reaction of **2** with diethylacetylene. This clearly showed that the bicyclic Dewar benzene type compound **3h** is an intermediate upon the formation of the tetrasilabenzvalene derivative **4**, which is the final product of this reaction (Figure S25). The identity of **3h** was confirmed by signals in the ^{29}Si NMR at 95.4 ppm for the Si=Si double bond. In this experiment sharp signals were observed in the NMR spectra indicating negligible diradical character of **3h** and **4h**. Additionally, a H,H correlated ROESY NMR experiment revealed no exchange signals and thus no equilibrium to exist between **3h** and **4h** (Figure S29). The formation of **4** can be explained with the significantly larger energy difference between the benzvalene compared to the Dewar benzene type isomer of 15.5 kcal mol^{-1}. Furthermore, we note that the difference in ΔG for **5** and the hypothetical bicyclic product is 14.2 kcal mol^{-1} in favor of **5**. This shows why we isolate the tricyclic product **5**.

The low difference in Gibbs free energy between **3e** and **4e** of only 3.1 kcal mol^{-1} suggests that valence isomerization between these two compounds might be achieved. Experiments in this direction show that **3** can only partially be converted into the tricyclic species **4e** upon thermal treatment of **3** at 60 °C for 19 h, which results in a 30:70 ratio of **4e** and **3**, respectively. Increasing the temperature leads to partial decomposition of **3** and **4e**. However, using visible light (LED, $\lambda = 405$ nm) in C_6D_6 results in complete photochemical conversion of **3** into **4e** within 1 h (Pages S34, S35). When **4e** is stored at room temperature in the dark slow isomerization back to **3** takes place in 18 days to result in a ca. 1:1 mixture of **3** and **4e**. Faster reconversion from **4e** to **3** occurs when **4e** is heated to 60 °C for 18 h to yield a 70:30 mixture of **3** and **4e**, respectively. A similar kind of interconversion between a digermabenzene and digerma-Dewar-benzene was recently reported.[30] Variable temperature and H,H ROESY NMR spectroscopy of the mixture of **3** and **4e** in [D_8]THF does not give evidence for an equilibrium between these two compounds (Figure S47, S48). Furthermore, we note that no change in the reaction was observed upon addition of 9,10-dihydroanthracene as trapping agent during the isomerization of **3** and **4e** with LED light (Scheme 4).

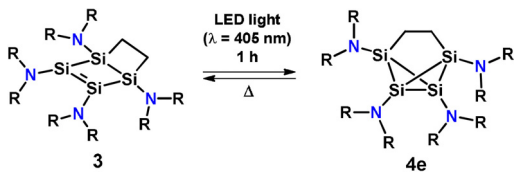

Scheme 4. Photochemical isomerization of **3** into **4e** and partial thermal reconversion to **3**.

Similar to the reaction with ethylene, the bicyclic product **6** from the reaction with 2,3-dimethyl-1,3-butadiene is almost identical in energy to the corresponding tricyclic compound ($\Delta G = 0.5$ kcal mol^{-1}, Table S22), and the reaction stops upon the formation of the thermodynamically slightly favored bicyclic product **6** at room temperature. In this case, conversion into the expected tricyclic product does not occur at elevated temperature (80 °C for 16 h). Irradiation of **6** with LED light ($\lambda = 405$ nm) for 1 h results in the formation of a new compound in ca. 80 % yield that is not the anticipated tricyclic product corresponding to **4e**. Instead [2+2] cycloaddition between the two double bonds in **6** occurred to afford **6′** (Figure S54).

In summary, we report on the reductive debromination of $\{N(SiMe_3)_2\}SiBr_3$ with Mg* that results in a 1:1 mixture of a five-vertex silicon cluster **1** and a tetrasilacyclobutadiene analogue **2** with a charge-separated electronic situation. Cycloadditions of **2** with ethylene, diethylacetylene, 1,5-cyclooctadiene and 2,3-dimethyl-1,3-butadiene at room temperature result in quantitative reactions to unsaturated bicyclic or tricyclic silicon ring species **3**–**6** with flexibility in the Si_4 unit to possess a tetrasilacyclobutene-type or a folded bicyclobutane-type structural motif. The product of each cycloaddition carried out at room temperature strongly depends on the Gibbs free energy difference between the bicyclic and the tricyclic isomers. With a larger difference in ΔG the thermodynamically more stable tricyclic product is formed in the case of **4** and **5**. Furthermore, we used light to perform selective photochemical isomerization when both isomers had very similar energy. In the case of **3** this was achieved with 405 nm LED light producing **4e**. When **6** was exposed to the same light source [2+2] cycloaddition between the two double bonds was observed to yield **6′**. Further reactivity studies with **2** will be pursued in our laboratory.

Acknowledgements

We thank the DFG (Heisenberg-Programm to F.L. and IRTG 2027 Münster Toronto support for M.F.) and the Boehringer Ingelheim Foundation (Exploration Grant to F.L.) for financial support. Tabea Rohlfs and Michael Quest are acknowledged for their help with the synthesis of **2** and **3**, respectively. We are grateful to Prof. W. Uhl and Prof. F. E. Hahn for their generous support. Open access funding enabled and organized by Projekt DEAL.

Conflict of Interest

The authors declare no conflict of interest.

Keywords: charge separation · cycloaddition · photochemical isomerization · silicon amides · tetrasilacyclobutadiene

[1] T. Bally, *Angew. Chem. Int. Ed.* **2006**, *45*, 6616 – 6619; *Angew. Chem.* **2006**, *118*, 6768 – 6771.
[2] J. I.-C. Wu, Y. Mo, F. A. Evangelista, P. v. R. Schleyer, *Chem. Commun.* **2012**, *48*, 8437 – 8439.
[3] A. Kostenko, B. Tumanskii, Y. Kobayashi, M. Nakamoto, A. Sekiguchi, Y. Apeloig, *Angew. Chem. Int. Ed.* **2017**, *56*, 10183 – 10187; *Angew. Chem.* **2017**, *129*, 10317 – 10321.
[4] G. F. Emerson, L. Watts, R. Pettit, *J. Am. Chem. Soc.* **1965**, *87*, 131 – 133.
[5] R. Pettit, J. Henery, *Org. Synth.* **1970**, *50*, 21.
[6] L. Watts, J. D. Fitzpatrick, R. Pettit, *J. Am. Chem. Soc.* **1965**, *87*, 3253 – 3254.
[7] a) N. V. Shvydkiy, D. S. Perekalin, *Coord. Chem. Rev.* **2017**, *349*, 156 – 168; b) O. I. Afanasyev, A. A. Tsygankov, D. L. Usanov, D. S. Perekalin, N. V. Shvydkiy, V. I. Maleev, A. R. Kudinov, D. Chusov, *ACS Catal.* **2016**, *6*, 2043 – 2046.
[8] K. Suzuki, T. Matsuo, D. Hashizume, H. Fueno, K. Tanaka, K. Tamao, *Science* **2011**, *331*, 1306 – 1309.
[9] S.-H. Zhang, H.-W. Xi, K. H. Lim, C.-W. So, *Angew. Chem. Int. Ed.* **2013**, *52*, 12364 – 12367; *Angew. Chem.* **2013**, *125*, 12590 – 12593.
[10] J. Keuter, K. Schwedtmann, A. Hepp, K. Bergander, O. Janka, C. Doerenkamp, H. Eckert, C. Mück-Lichtenfeld, F. Lips, *Angew. Chem. Int. Ed.* **2017**, *56*, 13866 – 13871; *Angew. Chem.* **2017**, *129*, 14054 – 14059.
[11] T. Iwamoto, T. Abe, K. Sugimoto, D. Hashizume, H. Matsui, R. Kishi, M. Nakano, S. Ishida, *Angew. Chem. Int. Ed.* **2019**, *58*, 4371 – 4375; *Angew. Chem.* **2019**, *131*, 4415 – 4419.
[12] T. Nukazawa, T. Iwamoto, *J. Am. Chem. Soc.* **2020**, *142*, 9920 – 9924.
[13] T. Nukazawa, T. Kosai, S. Honda, S. Ishida, T. Iwamoto, *Dalton Trans.* **2019**, *48*, 10874 – 10880.
[14] K. Takanashi, V. Y. Lee, T. Matsuno, M. Ichinohe, A. Sekiguchi, *J. Am. Chem. Soc.* **2005**, *127*, 5768 – 5769.
[15] V. Y. Lee, K. Takanashi, T. Matsuno, M. Ichinohe, A. Sekiguchi, *J. Am. Chem. Soc.* **2004**, *126*, 4758 – 4759.
[16] S. Inoue, J. D. Epping, E. Irran, M. Driess, *J. Am. Chem. Soc.* **2011**, *133*, 8514 – 8517.
[17] X. Sun, T. Simler, R. Yadav, R. Köppe, P. W. Roesky, *J. Am. Chem. Soc.* **2019**, *141*, 14987 – 14990.
[18] U. Wannagat, K. Behmel, H. Bürger, *Chem. Ber.* **1964**, *97*, 2029 – 2036.
[19] a) R. D. Rieke, *Science* **1989**, *246*, 1260 – 1264; b) R. D. Rieke, *Acc. Chem. Res.* **1977**, *10*, 301 – 306.
[20] a) P. P. Power, *Chem. Rev.* **1999**, *99*, 3463 – 3504; b) A. Sekiguchi, V. Y. Lee, *Chem. Rev.* **2003**, *103*, 1429 – 1448.
[21] M. D. Peeks, H. L. Anderson, *Chem* **2019**, *5*, 9 – 17.
[22] a) T. Yanai, D. P. Tew, N. C. Handy, *Chem. Phys. Lett.* **2004**, *393*, 51 – 57; b) S. Grimme, J. Antony, S. Ehrlich, H. Krieg, *J. Chem. Phys.* **2010**, *132*, 154104; c) S. Grimme, S. Ehrlich, L. Goerigk, *J. Comput. Chem.* **2011**, *32*, 1456 – 1465; d) F. Weigend, R. Ahlrichs, *Phys. Chem. Chem. Phys.* **2005**, *7*, 3297 – 3305.
[23] a) B. O. Roos, P. R. Taylor, P. E. Sigbahn, *Chem. Phys.* **1980**, *48*, 157 – 173; b) B. O. Roos, *Advances in Chemical Physics*, Wiley, Hoboken, **2007**, pp. 399 – 445.
[24] Q. Manh Phung, K. Pierloot, *Phys. Chem. Chem. Phys.* **2018**, *20*, 17009 – 17019.
[25] A. E. Reed, R. B. Weinstock, F. Weinhold, *J. Chem. Phys.* **1985**, *83*, 735 – 746.
[26] I. Mayer, *Chem. Phys. Lett.* **1983**, *97*, 270 – 274.
[27] K. Takanashi, V. Y. Lee, M. Ichinohe, A. Sekiguchi, *Chem. Lett.* **2007**, *36*, 1158 – 1159.
[28] N. Nakata, T. Oikawa, T. Matsumoto, Y. Kabe, A. Sekiguchi, *Organometallics* **2005**, *24*, 3368 – 3370.
[29] Deposition Numbers 2072552 (for **1**), 2072553 (for **2**), 2072554 (for **3**), 2072556 (for **4**), 2071559 (for **5**), and 2071560 (for **6**) contain the supplementary crystallographic data for this paper. These data are provided free of charge by the joint Cambridge Crystallographic Data Centre and Fachinformationszentrum

Karlsruhe Access Structures service www.ccdc.cam.ac.uk/structures.

[30] T. Sugahara, J.-D. Guo, D. Hashizume, T. Sasamori, N. Tokitoh, *J. Am. Chem. Soc.* **2019**, *141*, 2263 – 2267.

Manuscript received: March 29, 2021
Revised manuscript received: June 28, 2021
Accepted manuscript online: July 13, 2021
Version of record online: August 31, 2021

